Analysis and Computation using GTD of a Conducting Surface of Paraboloid Reflectors

Ajay Babu M.
Research scholar
Department of ECE,
CMJ University, India

Habibulla Khan, PhD.
Professor and HOD
ECE Dept.,
KL University, India

ABSTRACT
The Diffraction coefficient for electromagnetic waves incident obliquely incident on a curved edge formed by perfectly conducting plane surfaces. This diffraction coefficient remains valid in the transition region adjacent to shadow and reflection boundaries where the diffraction coefficients of Keller's original theory fail. Our method is proposed on Keller's method of the canonical problem, which in this case is the perfectly conducting wedge illuminated by plane, cylindrical, conical, and spherical waves. The expressions for the acoustic wedge diffraction coefficients contain Fresnel integral, which ensure that the total field is continuous at shadow and reflection boundaries. Since the diffraction is a local phenomenon, and locally the curved edge structure is wedge shaped, this result is readily extended to the curved wedge. It is interesting that even though the polarizations and the wavefront curvature of the incident, reflected, and diffracted waves are markedly different, the total field calculated from this high frequency solution for the curved wedge is continuous at shadow and reflection boundaries. The Jacoby polynomial series method, which has been demonstrated to provide an efficient means for evaluating the radiation integral of symmetric paraboloid. The analysis leading to the series formula is also useful for deriving an analytic expression for the optimum scan plane for the displacement of the feed. Representative numerical results illustrating the application of the method and the properties of the offset paraboloid are presented.

Keywords
Diffraction, Wedge, Dyads, Grazing, Offset, Jacobi polynomials.

1. INTRODUCTION
This paper deals with the construction of high-frequency solution for the diffraction of an electromagnetic wave obliquely incident on a smooth curved perfectly conducting surface surrounded by an isotropic homogenous medium. The surface normal is discontinuous at the edge and the two surfaces forming the edge may be convex, concave, or plane. The solution is developed within the context of Keller's geometrical theory of diffraction (GTD) [1]-[3] so the dyadic diffraction coefficient is of interest. Particular emphasis is placed on finding a compact accurate form of the diffraction coefficient valid in the transition regions adjacent to shadow and reflection boundaries and useful in practical applications. According to the GTD, a high frequency electromagnetic wave incident on an edge in a curved surface gives rise to a reflected wave, an edge diffracted wave, and an edge excited wave which propagates along a surface ray. Such surface ray fields may also be excited at shadow boundaries of the curved surface.

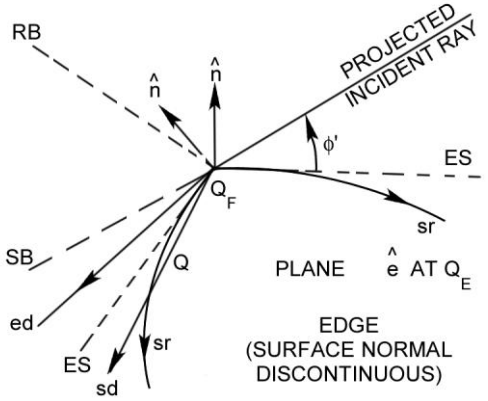

Fig.1 Illustrative view of Incident, Reflected, and Diffracted rays.

Fig.1 shows a plane perpendicular to the edge at the point of diffraction Q_E. The pertinent rays and boundaries are projected onto this plane. To simplify the discussion of the reflected field, we have assumed that the local interior wedge angle is $\leq \pi$. According to Keller's generalized Fermat's principle, the ray incident on the edge Q_E produces edge diffracted rays *ed* and surface diffracted rays *sr*. In the case of convex surfaces, the surface ray sheds a surface diffracted ray *sd* from each point *Q* on its path. *ES* is the boundary between the edge diffracted rays and the surface diffracted rays; it is tangent to the surface at Q_E. *SB* is the Shadow Boundary of the reflected fields, referred to, henceforth, simply as the reflection boundary. In present analysis it is assumed that the sources and field point are sufficiently removed from the surface and the boundary *ES* so that the contributions from the surface ray field can be neglected. The total electric field may then be represented as

$$E=E^i u^i + E^r u^r + E^d \quad (1)$$

In which E^i is the electric field of the source in the absence of the surface, E^r is the electric field reflected

from the surface with the edge ignored, and *Ed* is the edge diffracted electric field. The functions u^i and u^r are unit step functions which are equal to one in the regions illuminated by the incident and reflected fields and to zero in their shadow regions. The extent of these regions is determined by geometrical optics. The step functions are shown explicitly in (1) to emphasize the discontinuity in the incident and reflected fields at the shadow and reflection boundaries, respectively. They are not included in subsequent equations for reasons of notational economy.

2. Analysis of Edge Diffracted Field

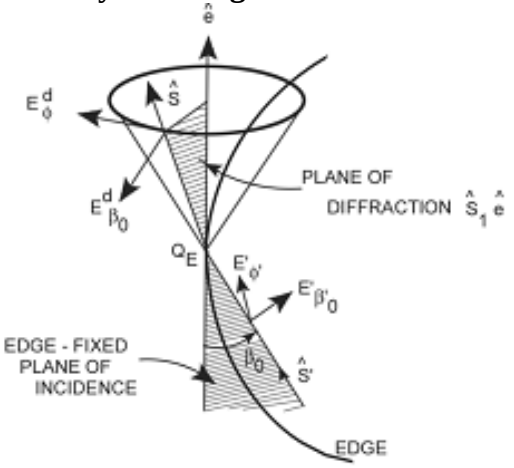

Fig. 2a

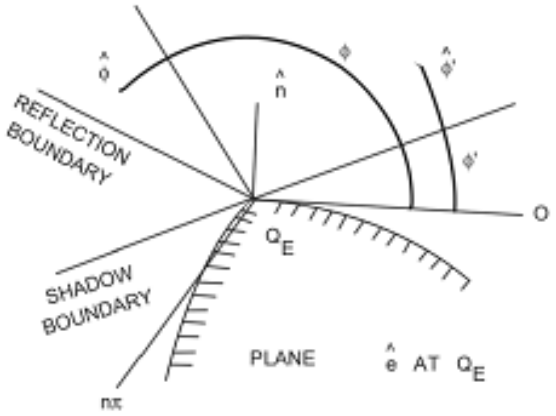

Fig. 2b Describes the Diffraction at a curved edge.

According to Keller's theory [3], the diffraction coefficient for a curved edge may be deduced from a two-dimensional canonical problem involving a straight edge, where the cylindrical surfaces which form the edge are defined by the boundary curves depicted in fig.2.(b). In the present discussion the edge may be an ordinary edge formed by a discontinuity in the unit normal vector, an edge formed by a discontinuity in surface curvature, or an edge formed by a discontinuity in some higher order derivative of the surface. Consider the z components of the electric and magnetic fields in the presence of this surface with an edge

$$E_z = E_z^1 + E_z^r + E_z^d \quad (2a)$$

$$H_z = H_z^1 + H_z^r + H_z^d \quad (2b)$$

They satisfy

$$\left(\nabla^2 + k^2\right)\begin{Bmatrix} E_z \\ H_z \end{Bmatrix} = 0 \quad (3)$$

Together with the soft (Dirichlet) or hard (Neumann) bound any conditions

$$E_z = 0 \quad (4)$$

$$\text{Or} \qquad \frac{\partial H_z}{\partial n} = 0 \quad (5)$$

respectively, on the boundary curve and the radiation condition at infinity. The $\frac{\partial H_z}{\partial n} = 0$ is the derivative along the normal to the boundary curve. Starting with the high frequency solutions for the z components of the diffracted field, substituting these into (3) and employing the methods described earlier, the asymptotic solutions may be put into the form

$$\begin{Bmatrix} E_z^d \\ H_z^d \end{Bmatrix} \sim \begin{Bmatrix} E_z^1 & D_s \\ H_z^i & D_h \end{Bmatrix} \sqrt{\frac{\rho}{s(\rho+s)}}\exp(-jks) \quad (6)$$

in which D_s, is referred to as the soft scalar diffraction, coefficient obtained when the soft boundary condition is used, and D_h is referred to as the hard scalar diffraction coefficient obtained when the hard boundary condition is used. Since

$$E_z^1 = E_{\beta_0^1}^1 \sin\beta_0 \quad (7a)$$

$$H_z^1 = Y_C E_\phi^1 . \sin\beta_0 \quad (7b)$$

and similarly for the z components of the diffracted field, it follows from (6) and (7) that

$$\begin{Bmatrix} E_{\beta_0}^d \\ E_\phi^d \end{Bmatrix} = - \begin{Bmatrix} E_{\beta_0^1}^1 & D_s \\ E_{\phi_1}^1 & D_h \end{Bmatrix} \sqrt{\frac{\rho}{s(\rho+s)}}\exp(-jks) \quad (8)$$

Consequently, the dyadic diffraction coefficient for an ordinary (or higher order) edge in a perfectly conducting surface can be expressed simply as the sum of two dyads

$$\bar{D} = -\hat{\beta}_0^1 \hat{\beta}_0 D_s - \hat{\phi}^1 \hat{\phi} D_h \quad (9)$$

to first order, since D_s, and D_h, are the ordinary scalar diffraction coefficients which occur in the diffraction of acoustic waves which encounter soft or hard boundaries, we see the close connection between electromagnetic and acoustics at high frequencies. The balance of this paper is concerned with finding expressions for D_s, and D_h, which can be used in the transition regions adjacent to shadow and reflection boundaries in the case of diffraction by an ordinary

edge. Recently, Keller and Kaminetzky [4] and Senior [5] have obtained expressions for scalar diffraction coefficients n the case of diffraction by an edge formed by a discontinuity in surface curvature, and senior [6] has given the dyadic diffraction coefficient in an edge-fixed coordinate system.

3. Analysis of the Wedge

The Bessel and Henkel functions in the Eigen function series are replaced by their integral representations and the series are then summed leaving the integral representations. Integral representations for the other field components in the edge fixed coordinate system are then found from the z (or edge) components, except in the case of the incident spherical wave, where the integral representations of the field components are obtained from the z components of the vector potentials, these integrals are approximated asymptotically by the Pauli-Clemmow method of steepest descent [7], and the leading terms are retained. If the field point is not close to a shadow or reflection boundary.

$$D_{s,h}(\phi,\ \phi^1;\ \beta_0)=\frac{\exp[-j(\pi/4)]\ \sin\pi/n}{n\sqrt{2\pi k}\ \sin\beta_0}$$

$$\cdot\left[\frac{1}{\cos\pi/n-\cos[(\phi-\phi^1)/n}\mp\frac{1}{\cos\pi/n-\cos[(\phi+\phi^1)/n]}\right] \quad (10)$$

Grazing incidence, where Φ'=o or nπ must be considered separately. In this case D_s =0, and the expression for D_h given by (10) must be multiplied by a factor of ½ . The need for the factor of ½ may be seen by considering grazing incidence to be the limit of oblique incidence. At grazing incidence the incident and reflected fields merge, so that one half the total field propagating along the face of the wedge toward the edge is the incident field and the other half is the reflected field. Nevertheless in this case it is clearly more convenient to regard the total field as the "incident" field. The factor of ½ is also apparent if the analysis is carried out with Φ'=0 or nπ.To simplify the discussion, the wedge angle has been restricted so that 1< n ≤2; however, the solution for the diffracted field may be applied to an interior wedge where 0 < n< 1. The diffraction coefficient vanishes where sin π/n =0; hence for n=1, the entire plane, n =1/2, the interior right angle, n=1/M, M=3,4,5,…., interior acute angles, the boundary value problem can be solved exactly in terms of the incident field and a finite number of reflected fields, which may be determined from image theory, moreover as n –> 0, even with the presence of a non-vanishing diffracted field, the phenomenon is increasingly dominated by the incident and reflected fields. In the transition regions the magnitude of the diffracted field is comparable with the incident or reflected field, and since these fields are discontinuous at their boundaries, the diffracted fields must be discontinuous at shadow and reflection boundaries for the total field to be continuous there. An expression for the dyadic diffraction coefficient of a perfectly conducting wedge which is valid both within and outside the transition regions [8] is provided by (9) with (10)

$$D_{s,h}(\phi,\ \phi^1;\beta_0)=\frac{-\exp[-j(\pi/4)]}{2n\sqrt{2\pi k}\ \sin\beta_0}$$

$$x\left[\cot\left(\frac{\pi+(\phi-\phi^1)}{2n}\right)F[KL\,a^+(\phi-\phi^1)]\right.$$

$$+\cot\left(\frac{\pi-(\phi-\phi^1)}{2n}\right)F(KL\,a^-(\phi-\phi^1)]$$

$$\mp\left\{\cot\left(\frac{\pi+\left(\phi+\phi^1\right)}{2n}\right)F(kL\,a^+(\phi+\phi^1)]\right.$$

$$\left.\left.+\cot\left(\frac{\pi-(\phi+\phi^1}{2n}\right)F(kL\,a^-(\phi+\phi^1)]\right\}\right] \quad (11)$$

Where

$$F(X)=2j\sqrt{X}\exp(jX)\int_{\sqrt{x}}^{\infty}\exp(-jr^2)dr \quad (12)$$

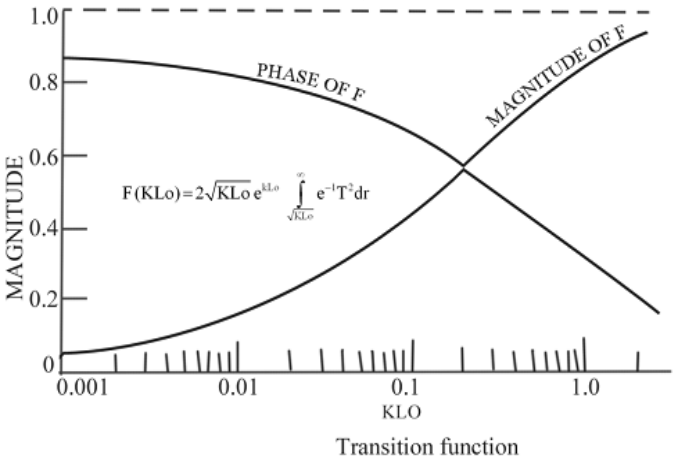

Fig. 3 Transition function

in which one takes the principal (positive) branch of the square root and

$$a^2(\beta)=2\cos^2\left(\frac{2n\pi N^2-(\beta)}{2}\right) \quad (13)$$

In which $N^{\pm}$ are the integers which most nearly equations.

$$2\pi nN^+-(\beta)=\pi \quad (14a)$$

And

$$2\pi nN^--(\beta)=-\pi \quad (14b)$$

With

$$\beta = \phi \pm \phi^1 \qquad (15)$$

It is apparent that N^+, N^- each has to values.

The preceding expression for the soft (s) and hard (h) diffraction coefficients contains a transition function F fined by (12) where it is seen that F(X) involves a integral. The magnitude and phase of F(X) are shown in fig. 3 where X=kLa. When X is small

$$F(X) - \left[\sqrt{\pi X} - 2X\exp\left(j\frac{\pi}{4}\right) - \frac{2}{3}X^2\exp\left(-i\frac{\pi}{4}\right).\exp\left[i\left(\frac{\pi}{4}+X\right)\right]\right] \qquad (16)$$

And When X is large

$$F(X) \sim \left(1 + j\frac{1}{2x} - \frac{3}{4}\frac{1}{x^2} - j\frac{15}{8}\frac{1}{X^3} + \frac{75}{16}\frac{1}{X^4}\right) \qquad (17)$$

If the arguments of the four transition functions in (11) exceed 10 it follows from the above equation that the transitions functions can be replaced by unity and (11) reduces to (10). L is a distance parameter, which was determined for se types of illumination. It was found that

$$L = \begin{cases} s\sin^2\beta_0 \\ \dfrac{rr^1}{r+r^{11}} \\ \dfrac{ss^1}{s+s^1}\sin^2\beta_0 \end{cases} \qquad (18)$$

The first response is for plane wave incidence, second for cylindrical – wave incidence, and the third for conical and spherical wave incidences. Where the cylindrical wave of radius r' is normally incident the edge, and r is the perpendicular distance of the field point from the edge.

4. Computation of Radiation Integral for the Offset Parabolic Reflector

The geometry of an offset reflector together with the location of the feed is shown. In Fig.4. The normalized radiation integral in terms of the induced current J on the surface of the reflector can be written as

$$E(0,\phi) = (\hat{I} - \hat{R}_0\hat{R}_0) \cdot \int\int_{\Sigma} Je^{-Jk(p'-p.R_0)}ds \qquad (19)$$

Where the optical phase of J has been factored out explicitly relative to an ideal phase center located at $\in$ (see Fig. 4). We also note that this integral is defined on the surface of the reflector. Often a ray-optical "approximation" is used to derive an alternative form for the radiation integral which requires the Fourier transformation of the truncated tangential fields on the projected aperture of the reflector, rather than on the reflector surface itself. However, as mentioned earlier, this introduces errors in the secondary pattern calculation at observation angles away from the main beam direction and is inaccurate for large beam displacements. We can, nevertheless, derive a mathematically exact form of (19) which is an integration over cylindrical coordinates which can be interpreted as projected aperture coordinates. This procedure is demonstrated in the following. Radiation integral (19) can be rewritten in terms of cylindrical coordinates (r,ϕ') of the "projected aperture" of the parent parabolic (see Fig. 4). We obtain for a typical scalar component of E, say $F(\theta,\phi)$, integrals of the type

$$F(0,\phi) = \iint g(r,\phi')e^{-Jk(\rho'-\rho.\hat{R}_0)}rdrd\phi' \qquad (20)$$

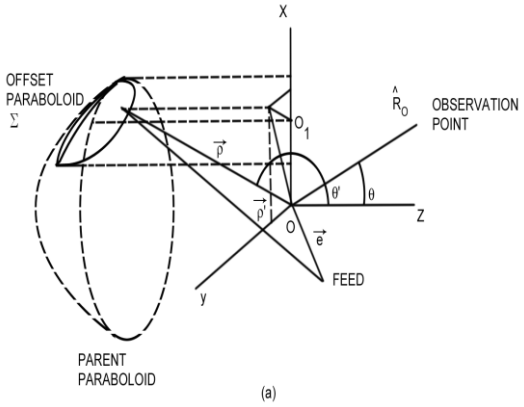

Three dimensional view.

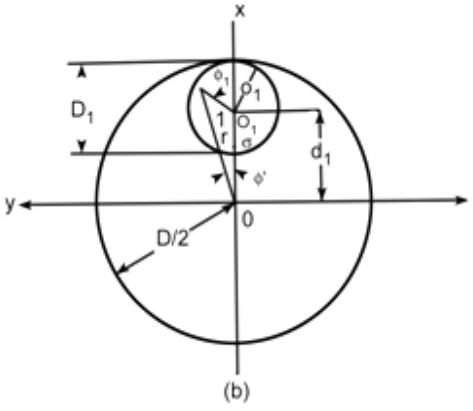

Projection on x-y plane.

Fig. 4. Geometry of offset paraboloid reflector antenna.

5. Result

The present approach is very well-suited for computing radiation patterns of large reflectors, even thousands of wavelengths in size. In fact, the relative advantages of the series method become even more evident when dealing with large reflector antennas, because the p series becomes more rapidly convergent as D/η is increased. Furthermore, the final result can be expressed in a scaled form, in terms of $(ka_1\eta_1,\alpha_1)$ such that the results for the pattern are relatively universal and independent of λ. These added features are quite useful when computing and displaying the radiation patterns. To demonstrate some representative results we consider a large offset paraboloid illuminated by displaced feeds. The geometry in shown in Fig. 4, and the reflector dimensions are

$$D/\lambda = 4533.33 \quad D_1/\lambda = 1866.67 \quad f/D = 1. \qquad (21)$$

Note that D. = parent paraboloid diameter, and $f/D_1 \cong 2$.These dimensions were chosen because of an interest at the Jet Propulsion Laboratory in computing the scan capabilities of large reflector antennas that may be erected in space in future applications. Furthermore, such a choice helps illustrate the computational efficiency and usefulness of the present approach even when the reflector size is very large. We have employed the Gauss-quadrature double integration scheme, as discussed in [9], to evaluate the integral. The required number of integration points are determined from the behavior of the function g_1, $\cos n\phi'$ and the modified Jacobi polynomials. For most cases studied in this work are quite well behaved, and Fig. 6. (a) clearly demonstrates that only 576 integration points suffice to yield accurate results. This is evident from the plots in Fig. 6. (a) which show that the results with 576 and 900 integration points are almost identical. Not unexpectedly, the required number of integration points increases with increasing M and N. For instance, for 8 < (M or N) < 14 one has to use at least 900 integration points in order to obtain accurate results.

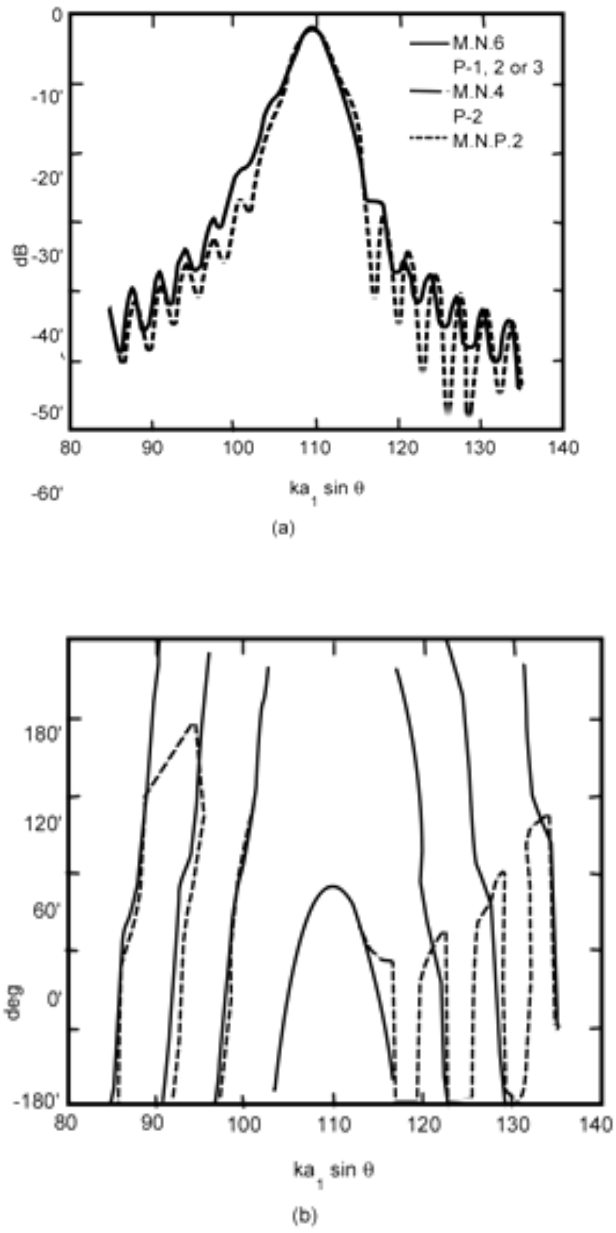

Fig. 5.(a) Amplitude of y component of far-field pattern in x-z plane for different P, N and M Reflector dimensions are given in (21). (b) Phase of y component of far-field pattern in x-z plane.

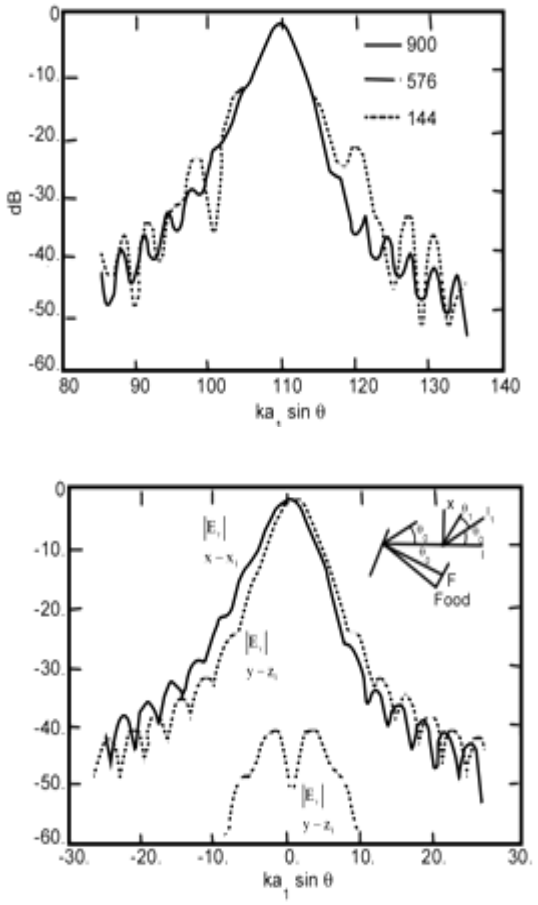

Fig.6. (a) Amplitude of y component of far-field pattern in x-z plane for different numbers of integration points (M=N=6, P=3). (b) Amplitude of y component (copolar) of far-field in x-z_1-and y-z_1-planes and amplitude of x component (cross polar) of far field in y-z_1 plane (ka1 sinθ1=110). Reflector dimensions are given in (21).

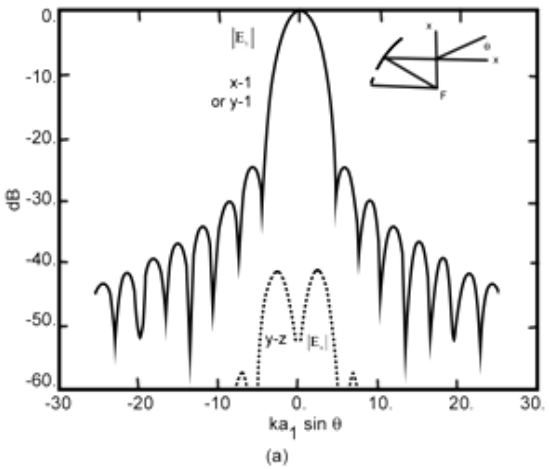

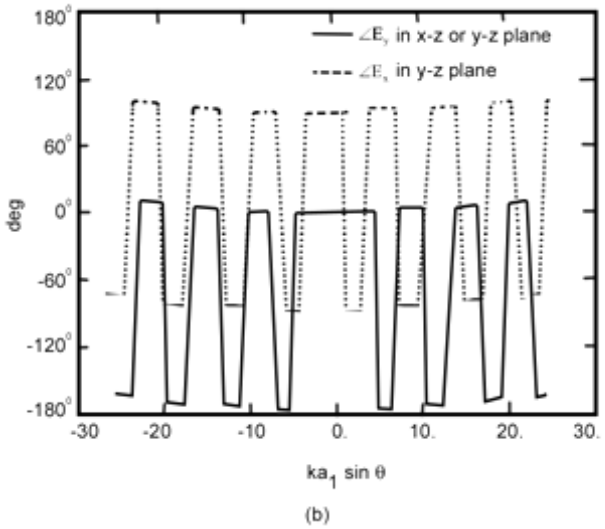

Fig. 7. (a) Amplitude of Y component (copular) of far field in X-Z – or Y-Z- planes, and amplitude of X component (cross polar) of far field in Y-Z- plane. $|E_x|$ in x-z- plane and $|E_z|$ in x-z and y-z-planes are negligible. Reflector dimensions are given in (21). (b) Phase of y component (copolar) of far field in x-z-or y-z-planes, and phase of x component (cross polar) of far field in y-z-plane.

6. CONCLUSION

It is interesting that even though the polarizations and the wavefront curvatures of the incident, reflected, and diffracted waves are markedly different, the total field calculated from this high-frequency solution for the curved wedge is continuous at shadow and reflection boundaries. Representative numerical results illustrating the application of the method and the properties of the offset paraboloid are present. Results obtained from the above assumptions would only be good for small f/D ratios and small beam width scans. New formulations for the offset geometry are an important subject for future study. For the sake of completeness we have used our general purpose computer program and generated most of the results reported in [10]. Our results compared very favorably with those given in [10], and in most cases considerably less computer time was needed in comparison with other techniques.

7. ACKNOWLEDGMENTS

We would like to express our thanks to the department of ECE and management of KL University for their continuous support and encouragement during this work. We also express our thanks to the department of ECE of CMJ University for providing lab facilities for the research work. Further author like to express sincere thanks to Prof. N.Venkatram, A/Dean, Electrical Sciences, KL University for providing

excellent R&D facilities at KL University to carry out this work.

8. REFERENCES

[1] J.B. Keller, "The geometric optics theory of diffraction," presented at the 1953 McGill SYMP. Microwave Optics, A.F. Cambridge Res. Cent., Rep. TR-59-118 (II), PP.207-210.1959.

[2] A geometrical theory of diffraction, in calculus of Variations and its Applications, L.M. Graves, Ed New York McGraw-Hill, 1958, PP.27-52.

[3] "Geometrical theory of diffraction," J. Opt. Soc. Amer., vol.52, pp 116-130, 1962.

[4] L. Kaminetsky and J.B. Keller, "Diffraction coefficients for higher order edges and vertices," SIAM J. Appl. Math., vol.22, pp.109-134, 1972.

[5] T. B. A. Senior. "Diffraction coefficients for a discontinuity in curvature," Electron. Lett., vol. 7. No. 10, pp.249-250, May,1971.

[6] T. B. A. Senior. "The Diffraction matrix for a discontinuity in curvature," IEEE Trans, Antennas Propagat., vol. AP-20, pp.326-333, May 1972.

[7] P.H. Pathak and R. G. Kouyoumjian, "The dyadic diffraction coefficient for a perfectly-conducting wedge," Electro Science Lab., Dep. Elec. Eng., Ohio State Univ., Columbus. June, 1970.

[8] P.C.Clemmow, Some extensions to the method of integration by steepest descents, Quart. J. Mech. Appl. Math., vol. 3, pp. 241-256, 1950

[9] M. Abramowitz and T. A. Stegun, Eds, Handbook of Mathematical Functions. New York: Dover, 1970, p. 892

[10] A. W. Love, Reflector Antennas. New York: IEEE, 1978.

AUTHOR'S PROFILE

M. Ajay Babu born in India in 1963. He did his B.Tech from KLCE in 1985 and M.Tech from JNTU Kakinada in 2000. He is pursuing his PhD in the field of Antennas from the CMJ University. He is having 28 years of teaching experience in various engineering colleges. He attended several workshops and seminars and he is having around 10 International Journal publications and Conference papers in his credit.

Dr. Habibulla Khan was born on August 11th, 1962. He received B.Tech from Nagrajuna University, in 1984 and M.E from Bharathier college of Engineering & Technology, in 1987. He awarded the PhD degree from Andhra University, Visakhapatnam in 2007. Currently he is working as Professor and Head of ECE Department, K L University. His current research interests include Slot Antenna, Communication Systems. He attended several workshops and seminars and he has published 55 papers in National and International Journals and presented 11 papers at National/International conferences. He published one book under the title of "Digital Logic Design". He is the Life Member of ISTE, SEMCE, IE, & Fellow IETE. Editorial board member of TIJCA, IJCEA, IJEAE and member board of Studies in ECE & EIE, Acharya Nagarguna University, India.